Title

ABCD of IA: A multi-scale agent-based model of T cell activation in inflammatory arthritis.

Journal

Biomaterials Science, 12(8)

Authors

McBride, David

Wang, James

Johnson, Wade

et al.

Publication Date

2024-04-16

DOI

10.1039/d3bm01674a

Peer reviewed

HHS Public Access

Author manuscript

Biomater Sci. Author manuscript; available in PMC 2025 January 23.

Published in final edited form as:

Biomater Sci. ; 12(8): 2041–2056. doi:10.1039/d3bm01674a.

ABCD of IA: A multi-scale agent-based model of T cell activation in inflammatory arthritis

David A. McBride[1,*], **James S. Wang**[1], **Wade T. Johnson**[1], **Nunzio Bottini**[2], **Nisarg J. Shah**[1,*]

[1]Department of NanoEngineering and Chemical Engineering Program, University of California, San Diego, La Jolla, CA 92093, USA

[2]Kao Autoimmunity Institute and Division of Rheumatology, Cedars-Sinai Medical Center, Los Angeles, CA 90048, USA

Abstract

Biomaterial-based agents have been demonstrated to regulate the function of immune cells in models of autoimmunity. However, the complexity of the kinetics of immune cell activation can present a challenge in optimizing the dose and frequency of administration. Here, we report a model of autoreactive T cell activation which are key drivers in autoimmune inflammatory joint disease. The model is termed a multi-scale Agent-Based, Cell-Driven model of Inflammatory Arthritis (ABCD of IA). Using kinetic rate equations and statistical theory, ABCD of IA simulated the activation and presentation of autoantigens by dendritic cells, interactions with cognate T cells and subsequent T cell proliferation in the lymph node and IA-affected joints. The results, validated with in vivo data from the T cell driven SKG mouse model, showed that T cell proliferation strongly correlated with the T cell receptor (TCR) affinity distribution (TCR-ad), with a clear transition state from homeostasis to an inflammatory state. T cell proliferation was strongly dependent on the amount of antigen in antigenic stimulus event (ASE) at low concentrations. On the other hand, inflammation driven by Th17-inducing cytokine mediated T cell phenotype commitment was influenced by the initial level of Th17-inducing cytokines independent of the amount of arthritogenic antigen. The introduction of inhibitory artificial antigen presenting cells (iaAPCs), which locally suppress T cell activation, reduced T cell proliferation in a dose-dependent manner. The findings in this work set up a framework based on theory and modeling to simulate personalized therapeutic strategies in IA.

[*]Corresponding authors: David A. McBride (d2mcbrid@ucsd.edu) and Nisarg J. Shah (nshah@ucsd.edu).

Author contributions:
Conceptualization: DAM, NJS
Methodology: DM, JSW, WTJ
Investigation: DAM, JSW, WTJ
Validation: DAM
Formal Analysis: DAM
Data Curation: DAM
Software: DAM
Visualization: DAM
Funding acquisition: DAM, NB, NJS
Project administration: NJS
Supervision: NB, NJS
Resources: NB, NJS
Writing – original draft: DAM, NJS
Writing – review & editing: DAM, JSW, WTJ, NB, NJS
All authors reviewed the data and analysis, provided input on the manuscript, and approved the submission.

Graphical Abstract

This study focuses on the development of a computational framework to simulate the contributing factors that lead to the evolution of autoreactive T cells in inflammatory arthritis. The results provide a tool for planning immunomodulatory strategies focused on new disease-modifying agents.

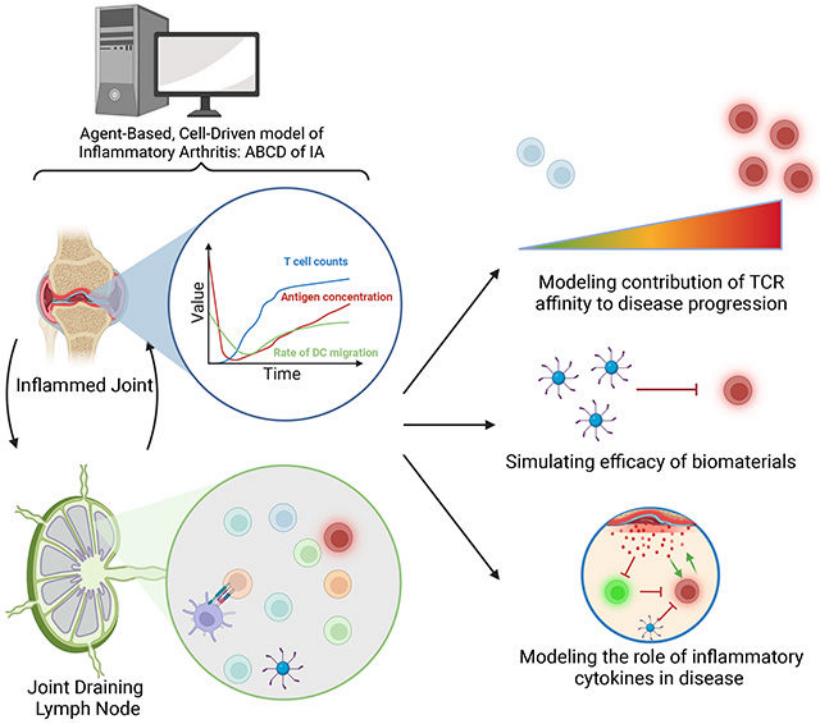

Keywords

modeling; autoimmunity; arthritis; biomaterials; immunomodulation

INTRODUCTION

Pathogenic inflammation of the joint, a hallmark of uncontrolled autoimmune inflammatory arthritis (IA) such as rheumatoid arthritis, is a common experience for patients and recapitulated in animal disease models. While the underlying causes are complex, a key contributing factor is the breakdown of regulatory mechanisms that typically restrain autoreactive T cells from inappropriate activation upon encountering self-antigens.(1,2) The hyperactivation of T cells feeds a cycle of chronic inflammation in the joint, which is correlated with damage of articular structures. (3–12) Even though biomaterials have been tested as immunomodulatory agents in models of arthritis and other autoimmune diseases, the complexity of immune activation make it challenging to determine the optimal therapeutic strategy to maximize clinical benefit.(13) Given the central role of T cell activation, a quantitative model describing the evolution of pathogenic T cells could help

better understand disease progression and inform the development of new biomaterial-based disease modifying agents.

To simulate the process of immune activation, agent-based models (ABMs) use a reductionist approach for understanding immune cell trafficking and predicting therapeutic efficacy and have been widely used for simulating immunological events in cancer and infectious disease.(14–17) In ABMs, the agents in the model represent cells and are governed by rules of cellular interactions relevant to the disease.(18) By specifying the rules or parameters governing the agents such as cellular heterogeneity, cellular movement speeds, and cell-to-cell interactions, non-intuitive behaviors may be predicted for further experimental validation.(19–22) ABMs are especially useful for capturing emergent non-intuitive behaviors, which are phenomena that arise from individual component interactions but are not inherently a rule of the individual components.(23–25) For example, ABMs have been particularly useful at modeling invasiveness and immune evasion of tumors that arise as a result of the individual properties of the cancer cells.(14,26) In IA, the degree of inflammation and tissue destruction are considered to be emergent properties resulting from the interaction of agents across multiple physiological compartments.(27) Thus, modeling inflammatory disease may be approached by integrating an ABM governing cellular agents with multiscale modeling across relevant length scales to account for communication between biological compartments as well as intracellular processes. The resulting model operates based on dynamics at the cellular and organ level to capture disease-relevant phenomena.

We focused on the T cell receptors (TCRs) that are associated with pathogenic T cells specific to autoantigens involved in disease.(8,28) TCRs recognize peptide fragments of autoantigens that are taken up, processed and presented by antigen presenting cells such as dendritic cells (DCs).(29,30) In IA, DCs may take up antigen at various extra- and intra-articular locations and typically traffic to lymph nodes to activate cognate T cells.(29) DCs also play a role in the development of ectopic lymphoid tissue in the joints of IA patients, which is associated with disease progression.(31) DC activation of T cells leads to clonal expansion of high affinity TCRs and an expansion of disease-specific T cells that drives the autoimmune response.(2,5) Hence, we focused on simulating interactions between T cells and autoantigen presenting DCs to understand how T cell activation by DCs contributes to disease pathogenesis.

We developed a multi-scale Agent-Based, Cell-Driven model of IA (ABCD of IA) which captures T cell and DC interactions in representative lymph node units (LNUs) and a joint compartment to which activated pathogenic T cells are recruited. By testing a range of TCR affinity distributions (TCR-ad), representing different possible TCR repertoires, and modulating the concentration of a burst release of antigen, referred to as an antigenic stimulus event (ASE), we determined how these factors influence pathogenic T cell proliferation. We found that the initial TCR-ad was a key contributing variable to pathogenic T cell proliferation. The TCR-ad and the initial antigen concentration following the ASE influenced both the level of proliferation and a corresponding pathogenic shift in the final TCR-ad. We simulated the introduction of a biomaterial-based immunomodulatory agent in the form of an inhibitory artificial APC (iaAPC) to modulate T cell activation and inhibit

proliferation directly in the LNU, representing emerging biomaterial-based lymph node targeted therapeutic strategies.(32,33) The iaAPCs operate based on principles of immune suppression of known immunosuppressive ligands such as programmed death-ligand 1 (PD-L1) and Fas ligand (FasL) to locally inhibit T cell activation.(34,35) The introduction of iaAPCs at the initiation of the simulation effectively inhibited pathogenic T cell proliferation in a concentration-dependent manner, with the minimum effective concentration dependent on the TCR-ad of the LNU.

METHODS

2.1 - Outline of Agent-Based Model

We sought to develop an agent-based model that recapitulates immune cell dynamics in the lymph node and associated joint that are affected by inflammation. We focused on the dynamics of T cell activation and proliferation in the lymph node during exposure to an autoantigen. 100 LNU simulations were run for each condition examined to account for the stochasticity of the model arising from the movement and interaction of the cellular agents. The model was run for a simulation time of eight days to assess. A functional outline of the model is presented here, while primary design choices of the model and additional details of the model equations and parameters may be found in the supplemental methods. For convenience, we use the term model to refer to the conceptual framework for the reduction of the biology, while the term simulation refers to an actual instance of computationally implementing and testing the model.

Upon initialization of the model 100 T cells are placed randomly in voxels representing 216 cubic μm, or 6 μm in a given direction, on a lattice geometry constrained to a spherical volume defining the LNU based on a pre-determined T cell density according to prior reports.(36) TCR affinities for the autoantigen are then assigned to individual T cells by randomly sampling from a Maxwell distribution, meant to represent a non-normal distribution that becomes increasing right skewed with an increasing scale parameter as defined in the scipy.stats.maxwell documentation.(37) The joint compartment antigen concentration is then set to the value of the initial antigenic stimulus and the model is initiated.

Following this initialization, DCs are probabilistically recruited to the LNU based on the concentration of the antigen in the joint. When a DC is recruited, it is placed randomly in the LNU at an open lattice site. The DC soma, capable of interacting with T cells and stimulating them extends in an extended Moore neighborhood of a 3 voxel range in each direction, as others have previously reported.(38) The lifespan of a DC in the LNU is set upon entry for 44 ± 4 hours, after which the DC dies. DC recruitment is capped at one DC per 156 T cells.

Following the recruitment of DCs, cells are moved to new sites on the lattice. Due to their low velocity relative to T cells, DCs are considered to be stationary. T cells are moved to a random location within an extended Moores neighborhood of a 3-voxel range in each direction. To achieve this, the algorithm randomly lists all T cells, and then moves them one at a time to ensure that no cell is consistently constrained by moving last. To move the T

cells, a random open site in the extended Moores neighborhood is selected, and the T cell moves there. If no sites are open, the T cell does not move that time step.

Following the movement of cells, interactions are checked for and initiated between T cells and DCs. T cells that enter the soma of a DC experience a stimulation event and are immobile for a duration dependent on their stage of activation, as observed in vivo.(39,40) The amount of stimulation that a T cell receives during its stimulation event is proportional to the affinity of the T cell. Upon receiving sufficient stimulation, T cells progress through stimulation thresholds representing phases of activation and proliferate.(41)

Once a T cell reaches the threshold signal to begin proliferation, it takes approximately 18 hours to complete the proliferation event. Newly generated T cells are spawned next to the proliferating T cell at a randomly picked adjacent available lattice site. If no lattice site is available, the T cell waits until an adjacent lattice site is available to proliferate. The newly generated T cells have the same affinity parameter as the proliferating T cell. The new T cell inherits the affinity and other properties of the parent T cells. The parent and new T cell evenly split the amount of intracellular signal accumulated in the parent T cell.

After any proliferation events, the algorithm then checks to see if any T cells egress from the lymph node. T cells are checked to egress from the LNU probabilistically at a rate comparable to homeostatic measurements.(42,43) T cells are considered activated once they can proliferate. If an activated T cell egresses from the LNU, it traffics to the joint and contributes to the generation of additional antigen. If a T cell that is not activated egresses from the LNU, it does not migrate to the joint. T cells are added to the LNU probabilistically at the same rate as they egress. New T cells added are assigned an affinity randomly sampled from the original Maxwell distribution.

Following egress, the bounds of the LNU are updated. As the lymph nodes are known to swell during immune response due to increased T cell numbers, the bounds of the LNU scale to keep the density of T cells in the LNU constant. T cells that move outside of the bounds of the LNU are moved to the corresponding location on the opposite side of the LNU that their movement would have taken them to otherwise. Following boundary movement, the simulation timestep is updated, data is exported for the timestep, and the next timestep initializes with DC recruitment. This continues until the simulation is complete.

2.2 - Testing the Effects of TCR Affinity Distribution

To test the role of the TCR affinity distribution on T cell proliferation in the LNUs and antigen production in the joint, we initialized the model drawing TCR affinities from different Maxwell distributions. Maxwell distributions were used as they are a well characterized distribution that shifts to a higher mean and standard deviation as a function of system variables. While classically this distribution represents the velocity distribution of molecules based on weight and temperature, here the shifting of the distribution can be considered a function of genes related to disease susceptibility that influence the affinity of the TCR repertoire for an autoantigen or T cell signaling pathways. We initialized 100 LNUs for each distribution tested to observe the effects of the distribution on model outputs.

2.3 - Comparison to In Vivo Data

To compare the outputs of ABCD of IA with in vivo data, we used previously generated datasets from our group.(44,45) Briefly, arthritis was induced in SKG mice via injection of mannan. Mice were sacrificed on days 1, 5 and 7 following mannan injection. The joint-draining popliteal lymph nodes and the hind ankles were harvested. Lymph nodes were dissociated using a 70 micron cell strainer. Skin and bone was removed from joint tissue and remaining tissue was digested in collagenase for 1 hour. Cells were stained with fluorescent antibodies for 15 minutes at 4C and analyzed using flow cytometry on an Attune NxT (ThermoFisher). FCS files were analyzed using FlowJo and gated on Live/$CD45^+$/$CD4^+$ to enumerate $CD4^+$ T cell counts in the joints and lymph nodes. The in vivo data was scaled appropriately and the trend in $CD4^+$ T cell counts were compared.

For phenotype model calibration and comparison, ankle T cell phenotype data from SKG mice were estimated based on Bottini et. al.(46) Briefly, T cells were isolated using a similar process as described above. Following isolation, cells were stained intranuclearly to determine FoxP3 and RORγt expression, indicative of T_{reg} and Th17 phenotypes, respectively. Parameter estimation for the phenotypic model was based on steady state T_{reg} and Th17 counts in non-arthritic and chronic arthritis stage mice.

2.4 - Testing the Effects of Initial Antigenic Stimulus

To test the role of the initial antigenic stimulus on T cell proliferation in the LNUs, we initialized the model with different initial concentrations of antigen in the joint. We performed an initial parameter sweep between 0 and 40000 nM, guided by intra-articular concentrations used in murine antigen induced arthritis models, for the ASE that revealed that the effects of increased antigen concentration during the ASE mostly plateaued after 500 nM.(47) We performed a set of follow up simulations at lower antigen concentrations. To understand how initial antigenic stimulus influenced outcomes of LNUs with different TCR affinity distributions, we reran these tests for low, medium, and high affinity TCR distributions.

2.5 - Testing the Effects of iaAPCs

To test whether iaAPCs could constrain pathogenic T cell proliferation, we designed iaAPCs based on the principles of co-inhibitory T cell molecules such as PD-L1 and FasL. We implemented rules in which T cells that interacted with a iaAPC were not able to receive T cell signals via the TCR for up to 30 minutes. As T cell expressed co-inhibitory receptors tend to be upregulated upon initial T cell stimulus, T cells were only susceptible to iaAPC-mediated inhibition after reaching the first stimulation threshold. To understand how iaAPC-mediated inhibition might operate, we simulated a range of iaAPC concentrations relative to initial T cell counts and across various TCR affinity distributions. iaAPCs did not clear from the LNUs and no new iaAPCs were added after LNU initialization.

2.6 - Testing the Role of the Inflammatory Milieu in Transition to Chronic Arthritis

To test the role of T cell phenotype commitment and inflammatory signaling in the joint milieu, we incorporated a joint inflammation parameter and inflammation-dependent T cell phenotype commitment and function in the joint. Depending on the composition of

the cytokine milieu and cell intrinsic properties, T cells may take on pro-inflammatory or anti-inflammatory function, which contributes the rise of distinct disease associate T cell subsets in inflammatory arthritis.(48–50) To model this we incorporated a T cell phenotype commitment component to the joint compartment in which T cells probabilistically differentiate into pro-inflammatory (Th17) or anti-inflammatory (T_{reg}) cells in an inflammation-dependent manner. Parameters for probabilistic T cell differentiation were determined using reported experimental data.(44,46) In this addition to the model, Th17 cells contribute to inflammation and antigen production while T_{reg} cells promote inflammation resolution and prevent tissue damage and subsequent antigen production. To understand how initial inflammation levels influenced outcomes of LNUs we performed a parameter sweep across a range of initial inflammation states.

RESULTS

3.1 - Overview of ABCD of IA

We developed the ABCD of IA to capture the dynamics of pathogenic T cell expansion involved in the progression and flaring of IA. To this end, we created a multiscale computational representation of T cell activation and proliferation. The model consists of two distinct compartments, a lymph node unit (LNU) compartment and a joint compartment which interact via the migration of immune cells and antigen drainage (Figure 1a). The model is initialized with a specific TCR-ad from which the affinity of naïve T cells coming into the LNU are sampled, representing a specific TCR repertoire. At the start of the model, T cell proliferation is stimulated by a burst release of antigen, termed an antigenic stimulus event (ASE), in which an IA-relevant autoantigen is introduced into the model system in a source-agnostic manner. Subsequent autoantigen is released as a result of T cell driven inflammation in the joint compartment.

To capture T cell priming and activation, we modeled cell-to-cell interactions between DCs and T cells in a joint-draining lymph node (Figure 1b). As it was infeasible to simulate all lymph node cells in an ABM, the dynamics were modeled in a representative LNU with reduced cell counts relative to an entire lymph node. T cells in LNU were populated using the specified TCR-ad determined at simulation initialization which is based on a scaled Maxwell-Boltzman distribution, with the probability of observing a TCR with a given affinity for the autoantigen outlined in Equation 1.

$$P(x) = \sqrt{\frac{2}{\pi}} \frac{x^2 e^{-x^2/\left(2m^2\right)}}{m^3} \tag{1}$$

In this equation, P is the probability of observing a T cell with a TCR that has an affinity value (x) for the autoantigen. The parameter m determines the shape and mean of the TCR-ad, with a larger value of m producing a TCR-ad with a higher mean value.

For a given TCR-ad, the mean value of the TCR-ad provided a snapshot of the pathogenic potential of the T cells in the LNU. Hence, a low mean TCR-ad LNU represents a lymph

node in which T cells will probabilistically have a low affinity for the arthritogenic antigen while a high mean TCR-ad LNU represents a lymph node in which T cell are much more likely to have a high affinity for the antigen.

The model was also built to incorporate migration of activated T cells from the lymph node to a distal joint compartment representing a site of disease in IA (Figure 1c). The joint compartment was simulated using cell population-based differential equations. Activated T cells that migrated to the joint were assumed to mediate tissue destruction and autoantigen release at a level proportional to the number of infiltrated T cells in the joint compartment. This released autoantigen was then picked up by DCs in a probabilistic manner, after which antigen loaded DCs migrated back to the LNU to cyclically drive T cell proliferation.

In the LNU, T cell activation and proliferation occurred in stages based on accumulated stimulation level due to interactions with DCs (Figure 1d). We modeled three distinct stages of T cell maturation which include a rapid sampling stage, a long contact stage, and an activation and proliferation stage.(40) Model parameters and the levels of stimulation required for T cell stage transitions were based on experimental studies of T cell priming in the lymph node and prior work modeling T cell interactions in the lymph node.(1) Key simulation initialization parameters are summarized in Table 1.

To test a model immunomodulatory therapy, inhibitory artificial antigen presenting cells (iaAPCs) were designed in silico to transiently inhibit TCR signaling in a manner consistent with known TCR inhibitory pathways. To test their efficacy, iaAPCs were introduced concurrent with the ASE at various T cell:iaAPC ratios. T cells that reached the long contact stage of maturation upregulated co-inhibitory ligands after which the interaction between an iaAPC and the T cell resulted in the inhibition of signaling through the TCR for a short duration. To computationally implement the model, the input parameters were determined and input, after which all agents and compartments were initialized in the simulation. The algorithm built to implement the model operated by first updating the position of the agents, then determining which interactions between agents occur based on their status and position and implementing the interactions. The data from the timestep was then recorded and the simulation space was visualized (Figure 1e). This was repeated until the end of a prespecified simulation time, after which the data was exported and compiled for analysis. In this way, the ABCD of IA captures the kinetics of pathogenic T cell proliferation in response to an autoantigen.

While T cells are critical components that orchestrate the immune response in inflammatory arthritis, not all T cells are pro-inflammatory. Regulatory T cells (T_{reg}) act to control autoreactive T cells and resolve inflammation in otherwise healthy tissue. T cell phenotype commitment is and dependent on microenvironmental cues, including the presence of key inflammatory cytokines. To examine the role of T cell phenotype commitment in the joint, we introduced an additional inflammation parameter into the model and pro- and anti-inflammatory T cell subsets (Th17 and T_{reg} cells, respectively) into the joint compartment. In this version of the model, T cells commit to a phenotype following recruitment to the joint based on the level of inflammation in the joint, separate from the amount of antigen

present. Th17 cells contribute to inflammation and drive antigen generation, while T_{reg} cells inhibit Th17 cells and act to resolve inflammation and tissue damage.

3.2 Simulated LNUs capture differences in T cell proliferation in response to TCR affinity distribution.

To determine the role of the TCR-ad in driving pathogenic T cell proliferation, LNU initialized with T cells from increasingly arthritogenic TCR-ad were simulated (Figure 2a). LNU simulations initially consisting of 100 T cells were initialized with distributions that spanned low, medium and high TCR-ad (Figure 2b–c). Despite starting with the same number of initial T cells, LNUs initialized with high mean TCR-ad experienced significantly more T cell proliferation after 8 days than LNU with low or medium mean TCR-ad, while LNUs initialized with a very low mean TCR-ad experienced almost no T cell proliferation (Figure 2d, e). The number of T cells in the joint compartments of T cells with high mean TCR-ad paralleled the number of T cells in the LNU due to increased T cell migration from the LNU to the joint space (Figure 2f).

We compared model predictions to lymph node and ankle T cell counts in the T cell-driven SKG model of autoimmune arthritis from datasets previously generated and published by our group.(44,45) Comparison of model results to in vivo data showed that T cell proliferation in the lymph node follows a similar trend to model predictions in the range of m = 800 - 1000 TCR-ad values (Figure 2g). Ankle T cell counts follow a similar growth trend between the model and in vivo measurements, but in vivo measurements after day 1 or arthritis induction are higher than model predictions (Figure 2f).

3.3 Proliferation of high affinity T cells drives a pathogenic shift in the TCR-ad in the LNU.

Following the observation of differential T cell proliferation based on the initial TCR-ad of the LNUs, we then assessed the clonal expansion that drives a shift in the relative abundance of T cell clonotypes during inflammation. We first compared the change in the mean of TCR-ads at the beginning and end of the simulation. The initial mean values of the TCR-ad in LNUs with T cells associated with low and very low TCR affinity distributions were similar to their final mean values, indicating a similar initial and final TCR-ad in the LNUs (Figure 3a). In contrast, the mean value of the TCR-ad of LNUs initialized with medium and high initial mean TCR-ad increased over time, representing an increase in the fraction of T cells with a high affinity for the autoantigen. The observed shifts started earlier in higher mean TCR-ad LNUs (Figure 3b). Examination of the change over time of the means of the TCR-ad revealed that TCR-ad does not change for LNU with T cells sampled from TCR-ad with Maxwell-Boltzmann scale parameters below a threshold of m = 600. For LNU with T cells sampled from TCR-ad higher than this threshold, the ending mean value of the TCR-ad relative to the initial value increased proportionally to the initial mean values of the TCR-ad (Figure 3c).

3.4 Pathogenic T cell proliferation is dependent on the magnitude of the initial antigenic stimulus.

Next, we sought to correlate the magnitude of the initiating ASE and the resultant proliferation of pathogenic T cells. We initialized simulations with a range of antigenic

loads for LNUs with low, medium and high mean TCR-ad (Figure 4a, b). No shift was observed in the TCR-ad of low mean affinity LNUs, while a shift towards T cells with high autoantigen affinity was observed in the TCR-ad of LNUs initialized with high mean TCR-ad (Figure 4c). The degree of shift in the TCR-ad of an LNU was dependent on antigen concentration as well as the initial TCR-ad (Figure 4d). For LNUs initialized with low mean TCR-ad, the TCR-ad remained constant throughout the simulation, regardless of the magnitude of the ASE. The TCR-ad of LNUs initialized with medium mean TCR-ad were sensitive to the size of the ASE between 40 to 320 nM of antigen, with sizeable shifts in the mean value of the TCR-ad from the beginning to the end of the simulation. The TCR-ad of LNUs initialized with high mean TCR-ad were the most sensitive to the size of the ASE, with significant shifts in the mean TCR-ad value over the course of the simulation starting at 10 nM of antigen and increasing up to 80 nM, after which the magnitude of the shift plateaued. The amount of T cell proliferation in the LNUs followed a similar trend to TCR-ad shifts, with proliferation highly dependent on both initial TCR-ad and the magnitude of the ASE (Figure 4e). In low mean TCR-ad LNU, minimal T cell proliferation was observed, regardless of the size of the ASE. In medium mean TCR-ad, and ASE above 80 nM induced some proliferation though the amount of proliferation plateaued, and the most proliferative LNUs under this condition only experienced an approximately four-fold change in T cell counts (Figure 4e). For LNUs initialized with a high mean TCR-ad, T cell proliferation increased with antigen concentration even at low antigen concentrations, but again T cell counts plateaued at antigen concentrations above 320 nM for the ASE, albeit at a fold change of approximately seven-fold in T cell counts.

3.5 Inhibitory artificial antigen presenting cells effectively control disease-specific immune activation.

Next, we introduced iaAPCs in the simulation to measure control of pathogenic T cell proliferation. We tested the effect of the introduction of iaAPCs concurrent with the ASE on T cell proliferation in LNUs initialized with low, medium, and high mean TCR-ad (Figure 4a–d). At a ratio of 100:1 T cells:iaAPCs, proliferation was slightly diminished relative to no iaAPCs (Figure 5e). However, as the ratio decreased to 100:2, and 100:3, proliferation decreased but still represented a high level of T cell proliferation. At ratios of 100:8 and above, T cell proliferation in the LNU was highly suppressed regardless of the initial TCR affinity distribution. A similar trend was observed for LNUs with medium and low mean TCR-ad, though full suppression of proliferation was achieved at lower doses, a ratio of approximately 100:4 T cells to iaAPCs for the medium mean TCR-ad LNUs and 100:2 T cells to iaAPCs for the low mean TCR-ad LNUs. The suppression of proliferation was also reflected in the mean TCR-ad, as high ratios of iaAPCs maintained a consistent mean value of the TCR-ad over time (Figure 5f).

3.6 The cytokine milieu in the joint microenvironment drives transition to chronic inflammation over resolution.

To simulate the role of cytokine signaling and T cell function on the initiation of arthritis, we incorporated T cell phenotype commitment based on the level of Th17-inducing cytokines in the joint compartment model (Figure 6a), a distinct parameter from the amount of arthritogenic antigen and based on experimental data. The model was initialized

with different levels of Th17-inducing cytokines. At low initial levels of Th17-inducing cytokines, T cells underwent proliferation and recruitment to the joint. However, subsequent commitment to a T_{reg} phenotype inhibited further T cell proliferation and recruitment with minimal Th17 differentiation (Figure 6b–e). At intermediate levels of Th17-inducing cytokines, Th17 differentiation was observed, driving a prolonged inflammatory response, but inflammation was ultimately resolved. At high levels of Th17-inducing cytokines, T_{reg} were unable to control Th17-driven inflammation and T cell proliferation led to uncontrolled inflammation, indicating a transition towards a chronically inflamed state.

We then modeled the introduction of iaAPC in a high Th17-inducing cytokine environment (I = 10000). In the absence of iaAPC, T cell proliferation was uncontrolled in the LNU (Figure 6f) accompanied by additional recruitment of T cells to the joint compartment (Figure 6g). The T_{reg}:Th17 ratio in the joint skewed towards a range that represented chronic inflammation (Figure 6h–i). At an initial T cell:iaAPC ratio of 100:2, T cell proliferation was controlled after an initial transient increase, and Th17 cells were no longer present in the joint by the end of the 8 days of simulation. With increasing relative initial amounts of iaAPC, T cell proliferation was rapidly controlled, with attenuation of joint infiltrating T cells. These results support the potential of ABCD of IA to model dose-dependent efficacy of novel T cell-modulating therapeutic strategies.

DISCUSSION

Here, we applied the principles of multiscale and agent-based models to develop the ABCD of IA, which simulate pathogenic T cell proliferation in IA. We probed the role of the TCR repertoire, autoantigen release and cytokine concentrations in disease transition to an inflamed state. We found that the TCR-ad strongly influenced T cell proliferation, with higher mean TCR-ads resulting in greater amounts of T cell proliferation while a low enough mean TCR-ad experienced no T cell proliferation. TCR-ad in the LNU evolved, becoming more pathogenic as a result of expansion of high affinity T cells, paralleling the clonal expansions reported during immune responses in vivo. The amount of T cell proliferation was also sensitive to the amount of antigen introduced to the system during the ASE, although at high antigen concentrations T cell proliferation plateaued. On the other hand, suppression of T cell proliferation by iaAPCs was dose dependent, with a higher dose of iaAPCs needed to control T cell proliferation in LNUs with higher mean TCR-ad. Independent of autoantigen concentration, cytokine levels can influence T cell polarization and drive inflammation. Overall, the development of the ABCD of IA provided insights into biological interactions that drive disease and the feasibility of a possible biomaterial-based therapeutic intervention, demonstrating the potential usefulness of ABCD of IA to further probe questions relating to pathogenic T cell expansion in IA.

ABCD of IA quantified the effect of the TCR repertoire and clonal expansion of arthritogenic T cells might play in driving disease susceptibility. For low mean TCR-ad, expansion of pathogenic T cells was not observed regardless of the amount of antigen released in the ASE. In contrast, high mean TCR-ad had some amount of pathogenic T cell expansion, even at low concentrations of antigen, suggesting that the TCR affinities are a key factor in determining the development of inflammation due to autoantigen release. This

finding is in line with results from animal models and human studies of the role of the TCR repertoire in the development of IA. For example, in the SKG mouse model of autoimmune arthritis, T cell driven joint inflammation arises due to a defect in T cell signaling which alters the TCR repertoire and generates a higher frequency of arthritogenic T cells.(13,51) In humans, specific human leukocyte antigen (HLA) alleles, the human version of MHCs, are closely linked with disease susceptibility in humans in a manner that likely has to do with how this shapes the TCR repertoire and which antigens are presented to T cells.(28,52,53) Our findings corroborate that alterations in the TCR repertoire that result in a greater frequency of T cells with a high affinity for an autoantigen can drive pathogenic T cell proliferation and that disease severity correlates with an oligoclonal expansion of joint-specific T cells, which has also been demonstrated in human disease.(54)

The dynamics of T cell activation modeled by ABCD of IA are well supported by prior in vivo results from arthritic SKG mice.(44,45) Prior work from animal models has established that activated DCs contribute to the development of IA pathology.(55) Adoptive transfer of autoantigen-primed DCs have been shown to expand disease-specific T cells in the joint-draining lymph node in mice.(56) On the other hand, *Batf3*$^{-/-}$ mice, which have defective DCs and exhibit impaired antigen cross-presentation in the lymph node, are resistant to autoimmune arthritis.(57) DCs can also infiltrate synovial tissue and fluid and often cluster with T cells in tertiary lymphoid-like structures. Such DC can process and present joint autoantigens and polarize T cells into pro-inflammatory phenotypes, contributing to disease progression.(58) Lymph nodes are not the sole source of arthritogenic T cells and resident memory T cells can also contribute to joint inflammation.(3,6) When compared with in vivo data from the SKG mouse model, increase of T cells in the joints was observed to be more rapid than the model prediction immediately following arthritis induction. This difference suggests that in the early stage of the disease, T cell migration from the lymph node is augmented by recruitment from other sources such as circulating T cells, tissue-resident T cells or by local expansion in the joint of SKG mice. ABCD of IA more closely models the later stage dynamics of T cell accumulation in the inflamed joint. ABCD of IA accurately predicts T cell expansion in the lymph node over the simulation timeframe.

ABCD of IA conducted a sensitivity analysis of pathogenic T cell proliferation to the amount of antigenic stimulus. The amount of T cell proliferation observed in the LNUs was highly dependent on the initial antigen concentration of the ASE at low concentrations, but quickly reached a maximal level of proliferation regardless of how high of a concentration of antigen was present. The plateau effect may be due, at least in part, to constraints placed on the number of DCs allowed to migrate into the lymph node based on the number of DCs in the lymph node. The specific antigen concentrations at which T cell proliferation in the model plateaus are comparable to antigen levels used to induce inflammation via antigen-specific T cell responses in mouse models.(3,59) Furthermore, higher mean TCR-ad LNUs had a lower threshold to reach high levels of T cell proliferation. This observation is consistent with the concept that genetic variations that shape antigen presentation and the TCR repertoire are major contributors to IA susceptibility.(1,28) The observation that low mean TCR-ad LNUs experience some T cell proliferation and shift towards a higher mean TCR-ad may explain how repeated ASE may slowly shift an IA prone individual to a chronically inflamed state. This is consistent with the concept that the exposome, defined

by an individual's history of environmental exposures, plays a large role in the development of IA.(60) As the initial ASE in the model is agnostic to antigen source, it is reasonable to include non-joint sources of antigen. As an example, it has been established that disruption of mucosal surfaces significantly increase the risk of developing IA, in part due to the generation of citrullinated peptides which are recognized by both B and T cells in disease.(61,62)

Even though TCR-signaling strength generally correlates with pMHC binding affinity, exceptions exist in which affinity alone may be inadequate in explaining all T cell functional outcomes. In particular, the acquisition of catch bonds within the TCR-pMHC interface has been shown to be a parameter that can permit differentiation between agonist from non-agonist ligands in the context of high-affinity TCR-pMHC interactions.(63–65) Prior work has developed models in the context of known peptides (e.g., from virus and cancer antigens) and TCR clones that are responsive (or not responsive) to pMHC. While these analyses do not include inflammatory arthritis (IA), we acknowledge that it is plausible that catch bonds influence T cell activation in IA. However, a major challenge with modeling catch bonds in inflammatory arthritis is that the participating antigens in humans are not known and therefore using ABCD of IA to validate the role of catch bonds in high-affinity TCR-pMHC interactions is currently not feasible.

The cytokine milieu in the joint microenvironment is an important determinant of T cell function. The role of cytokines that promote T_{reg} or Th17 differentiation is well established, which can alleviate or enhance disease respectively. (44,46,50,66) We simulated the role of cytokine-mediated T cell phenotype commitment using the ABCD of IA. The results showed that the persistence of inflammation was influenced by the initial level of Th17-inducing cytokines independent of the amount of arthritogenic antigen. This is consistent with experiments that demonstrate that sustained presentation of antigen in the absence of inflammation or in a tolerogenic environment confers disease protection in models of IA.(67–69) The model could be used to simulate the potential efficacy of biomaterial-based strategies that seek to reduce or eliminate pro-inflammatory cytokines or enhance immunoregulatory cell subsets through cytokine delivery.(44,45,70,71)

We also used the ABCD of IA to validate the concept of inhibiting T cell signaling to control T cell activation using iaAPCs. Because the effect of iaAPCs in inhibiting pathogenic T cell proliferation is concentration dependent, the appropriate dose for such a therapy would likely require careful dose titration. The precise dose to achieve disease control is dependent on an individuals' TCR-ad. The approach simulated here seeks to harness pre-empt inflammation and is aligned with similar strategies in experimental pre-clinical models of autoimmune disease.(72,73) However, translation of a strategy targeting T cells in lymph nodes will require additional materials engineering optimization to localize the effect of iaAPCs on pathogenic T cells while avoiding generalized immune suppression. Lessons learned from the study of tolerogenic dendritic cells will be invaluable for crafting biomaterials to inhibit specific T cell clonotypes and promote restoration of regulatory pathways to treat disease.(74,75)

As with any model of complex biological phenomena, it is important to note the assumptions used in the ABCD of IA where definitive biological data are not available. The simplification of T cell activation to a signal integration based on T cell avidity and DC interactions is necessary for agent-based modeling of T cells at scale while allowing for retention of key aspect of digital “on-or-off” T cell activation. As the direct measurement of all intracellular species involved in T cell activation is not possible, we used a previously reported intracellular model.(36) To determine the T cell avidities, we sampled from Maxwell distributions as exemplary right skewed distributions. Following a parameter sweep of distributions, we focused our investigation on the range of distributions that transitioned from low to high levels of T cell proliferation. The results of the simulation capture important aspects of inflammation in IA, including sensitivity to the autoantigen concentration, susceptibility associated with the TCR repertoire, and chronic T cell activation.

Biomaterial regulators of immunity have been widely used to modulate inflammation in models of autoimmune disease including arthritis. These include strategies that seek to scavenge pro-inflammatory cytokines or enhance immunoregulatory cell subsets through delivery of small molecules and cytokines.(44,45,70,71,76–78) A key optimization challenge of such agents is the determination of when to apply the therapeutic intervention. Because the cascade of immune activation is complex, suboptimal timing and delivery could result in low efficacy despite robust engineering of the therapeutic. To this end, simulations using ABCD of IA provide a potential tool to correlate key disease-relevant parameters that drive T cell-mediated pathogenesis in IA, thereby providing a window for optimal therapeutic intervention. ABCD of IA also provide a tool to simulate disease evolution, including transitions to a chronic state. The results provide a means to generate hypotheses relating to the screening the efficacy of biomaterial-based therapeutic strategies and potentially improve the efficiency of preclinical studies that are necessary for the development of disease-modifying drugs.

Supplementary Material

Refer to Web version on PubMed Central for supplementary material.

Acknowledgments

The authors acknowledge support from the Microenvironment in Arthritis Resource Center (MARC) at UC San Diego.

Funding:

National Institutes of Health grant F31AR079921 (DAM)

National Institutes of Health grant T32AR064194

National Institutes of Health grant P30AR073761 (NB)

National Institutes of Health grant R01AR081887 (NJS)

Arthritis National Research Foundation (NJS)

The content is solely the responsibility of the authors and does not necessarily represent the official views of the funding agencies, which includes the National Institutes of Health.

Data and materials availability:

All data are available in the main text or the supplementary materials. Code used to implement the model and run simulations is available at https://github.com/Shah-Lab-UCSD/LN_Model_Lattice.

References

1. Gravallese EM, Firestein GS. Rheumatoid Arthritis — Common Origins, Divergent Mechanisms. Longo DL, editor. N Engl J Med. 2023 Feb 9;388(6):529–42. [PubMed: 36780677]
2. McInnes IB, Schett G. The Pathogenesis of Rheumatoid Arthritis. N Engl J Med. 2011 Dec 8;365(23):2205–19. [PubMed: 22150039]
3. Chang MH, Levescot A, Nelson-Maney N, Blaustein RB, Winden KD, Morris A, et al. Arthritis flares mediated by tissue-resident memory T cells in the joint. Cell Reports. 2021 Oct;37(4):109902. [PubMed: 34706228]
4. Cope AP, Schulze-Koops H, Aringer M. The central role of T cells in rheumatoid arthritis. Clinical and Experimental Rheumatology. 2007;25.
5. Benson RA, Patakas A, Conigliaro P, Rush CM, Garside P, McInnes IB, et al. Identifying the Cells Breaching Self-Tolerance in Autoimmunity. The Journal of Immunology. 2010 Jun 1;184(11):6378–85. [PubMed: 20421640]
6. Hsieh WC, Svensson MND, Zoccheddu M, Tremblay ML, Sakaguchi S, Stanford SM, et al. PTPN2 links colonic and joint inflammation in experimental autoimmune arthritis. JCI Insight. 2020;5(20).
7. Long SA, Cerosaletti K, Wan JY, Ho JC, Tatum M, Wei S, et al. An autoimmune-associated variant in PTPN2 reveals an impairment of IL-2R signaling in CD4+ T cells. Genes Immun. 2011 Mar;12(2):116–25. [PubMed: 21179116]
8. Stanford SM, Bottini N. PTPN22: the archetypal non-HLA autoimmunity gene. Nat Rev Rheumatol. 2014 Oct;10(10):602–11. [PubMed: 25003765]
9. The Wellcome Trust Case Control Consortium. Genome-wide association study of 14,000 cases of seven common diseases and 3,000 shared controls. Nature. 2007 Jun;447(7145):661–78. [PubMed: 17554300]
10. Wiede F, Shields BJ, Chew SH, Kyparissoudis K, van Vliet C, Galic S, et al. T cell protein tyrosine phosphatase attenuates T cell signaling to maintain tolerance in mice. J Clin Invest. 2011 Dec 1;121(12):4758–74. [PubMed: 22080863]
11. Wiede F, Sacirbegovic F, Leong YA, Yu D, Tiganis T. PTPN2-deficiency exacerbates T follicular helper cell and B cell responses and promotes the development of autoimmunity. Journal of Autoimmunity. 2017 Jan;76:85–100. [PubMed: 27658548]
12. Nguyen CT, Maverakis E, Eberl M, Adamopoulos IE. γδ T cells in rheumatic diseases: from fundamental mechanisms to autoimmunity. Semin Immunopathol. 2019 Sep;41(5):595–605. [PubMed: 31506867]
13. Sakaguchi N, Takahashi T, Hata H, Nomura T, Tagami T, Yamazaki S, et al. Altered thymic T-cell selection due to a mutation of the ZAP-70 gene causes autoimmune arthritis in mice. Nature. 2003;426(6965).
14. Metzcar J, Wang Y, Heiland R, Macklin P. A Review of Cell-Based Computational Modeling in Cancer Biology. JCO Clinical Cancer Informatics. 2019 Dec;(3):1–13.
15. Glen CM, Kemp ML, Voit EO. Agent-based modeling of morphogenetic systems: Advantages and challenges. Castiglione F, editor. PLoS Comput Biol. 2019 Mar 28;15(3):e1006577. [PubMed: 30921323]
16. Kirschner D, Pienaar E, Marino S, Linderman JJ. A review of computational and mathematical modeling contributions to our understanding of Mycobacterium tuberculosis within-host infection and treatment. Current Opinion in Systems Biology. 2017 Jun;3:170–85. [PubMed: 30714019]

17. Wang Z, Butner JD, Cristini V, Deisboeck TS. Integrated PK-PD and agent-based modeling in oncology. J Pharmacokinet Pharmacodyn. 2015 Apr;42(2):179–89. [PubMed: 25588379]
18. Jenner AL, Smalley M, Goldman D, Goins WF, Cobbs CS, Puchalski RB, et al. Agent-based computational modeling of glioblastoma predicts that stromal density is central to oncolytic virus efficacy. iScience. 2022 Jun;25(6):104395. [PubMed: 35637733]
19. Yu JS, Bagheri N. Agent-Based Models Predict Emergent Behavior of Heterogeneous Cell Populations in Dynamic Microenvironments. Front Bioeng Biotechnol. 2020 Jun 11;8:249. [PubMed: 32596213]
20. Leighow SM, Landry B, Lee MJ, Peyton SR, Pritchard JR. Agent-Based Models Help Interpret Patterns of Clinical Drug Resistance by Contextualizing Competition Between Distinct Drug Failure Modes. Cel Mol Bioeng. 2022 Oct;15(5):521–33.
21. Zhang Z, Igoshin OA, Cotter CR, Shimkets LJ. Agent-Based Modeling Reveals Possible Mechanisms for Observed Aggregation Cell Behaviors. Biophysical Journal. 2018 Dec;115(12):2499–511. [PubMed: 30514635]
22. González-Valverde I, García-Aznar JM. Mechanical modeling of collective cell migration: An agent-based and continuum material approach. Computer Methods in Applied Mechanics and Engineering. 2018 Aug;337:246–62.
23. Hellweger FL, Clegg RJ, Clark JR, Plugge CM, Kreft JU. Advancing microbial sciences by individual-based modelling. Nat Rev Microbiol. 2016 Jul;14(7):461–71. [PubMed: 27265769]
24. Gorochowski TE, Hauert S, Kreft JU, Marucci L, Stillman NR, Tang TYD, et al. Toward Engineering Biosystems With Emergent Collective Functions. Front Bioeng Biotechnol. 2020 Jun 26;8:705. [PubMed: 32671054]
25. Prigogine I, Nicolis G. Self-Organisation in Nonequilibrium Systems: Towards A Dynamics of Complexity. In: Hazewinkel M, Jurkovich R, Paelinck JHP, editors. Bifurcation Analysis [Internet]. Dordrecht: Springer Netherlands; 1985 [cited 2023 May 2]. p. 3–12. Available from: http://link.springer.com/10.1007/978-94-009-6239-2_1
26. Norton KA, Popel AS. An agent-based model of cancer stem cell initiated avascular tumour growth and metastasis: the effect of seeding frequency and location. J R Soc Interface. 2014 Nov 6;11(100):20140640. [PubMed: 25185580]
27. Chavali AK, Gianchandani EP, Tung KS, Lawrence MB, Peirce SM, Papin JA. Characterizing emergent properties of immunological systems with multi-cellular rule-based computational modeling. Trends in Immunology. 2008 Dec;29(12):589–99. [PubMed: 18964301]
28. Jawaheer D, Seldin MF, Amos CI, Chen WV, Shigeta R, Monteiro J, et al. A Genomewide Screen in Multiplex Rheumatoid Arthritis Families Suggests Genetic Overlap with Other Autoimmune Diseases. The American Journal of Human Genetics. 2001 Apr;68(4):927–36. [PubMed: 11254450]
29. Yu MB, Langridge WHR. The function of myeloid dendritic cells in rheumatoid arthritis. Rheumatol Int. 2017 Jul;37(7):1043–51. [PubMed: 28236220]
30. Wehr P, Purvis H, Law SC, Thomas R. Dendritic cells, T cells and their interaction in rheumatoid arthritis. Clinical and Experimental Immunology. 2019 Mar 18;196(1):12–27. [PubMed: 30589082]
31. Corsiero E, Bombardieri M, Manzo A, Bugatti S, Uguccioni M, Pitzalis C. Role of lymphoid chemokines in the development of functional ectopic lymphoid structures in rheumatic autoimmune diseases. Immunology Letters. 2012 Jul;145(1–2):62–7. [PubMed: 22698185]
32. Tostanoski LH, Chiu YC, Gammon JM, Simon T, Andorko JI, Bromberg JS, et al. Reprogramming the Local Lymph Node Microenvironment Promotes Tolerance that Is Systemic and Antigen Specific. Cell Reports. 2016;16(11):2940–52. [PubMed: 27626664]
33. Gammon JM, Jewell CM. Engineering Immune Tolerance with Biomaterials. Adv Healthcare Mater. 2019 Feb;8(4):1801419.
34. Sugita S, Usui Y, Horie S, Futagami Y, Aburatani H, Okazaki T, et al. T-Cell Suppression by Programmed Cell Death 1 Ligand 1 on Retinal Pigment Epithelium during Inflammatory Conditions. Invest Ophthalmol Vis Sci. 2009 Jun 1;50(6):2862. [PubMed: 19182257]

35. Usui Y, Okunuki Y, Hattori T, Kezuka T, Keino H, Ebihara N, et al. Functional expression of B7H1 on retinal pigment epithelial cells. Experimental Eye Research. 2008 Jan;86(1):52–9. [PubMed: 17981268]
36. Bogle G, Dunbar PR. Agent-based simulation of T-cell activation and proliferation within a lymph node. Immunol Cell Biol. 2010 Feb;88(2):172–9. [PubMed: 19884904]
37. Virtanen P, Gommers R, Oliphant TE, Haberland M, Reddy T, Cournapeau D, et al. SciPy 1.0: fundamental algorithms for scientific computing in Python. Nat Methods. 2020 Mar 2;17(3):261–72. [PubMed: 32015543]
38. Bogle G, Dunbar PR. On-Lattice Simulation of T Cell Motility, Chemotaxis, and Trafficking in the Lymph Node Paracortex. Ploegh HL, editor. PLoS ONE. 2012 Sep 19;7(9):e45258. [PubMed: 23028887]
39. Textor J, Peixoto A, Henrickson SE, Sinn M, von Andrian UH, Westermann J. Defining the quantitative limits of intravital two-photon lymphocyte tracking. Proc Natl Acad Sci USA. 2011 Jul 26;108(30):12401–6. [PubMed: 21734152]
40. Mempel TR, Henrickson SE, von Andrian UH. T-cell priming by dendritic cells in lymph nodes occurs in three distinct phases. Nature. 2004 Jan;427(6970):154–9. [PubMed: 14712275]
41. Oh H, Ghosh S. NF-κB: roles and regulation in different CD4 $^{+}$ T-cell subsets. Immunol Rev. 2013 Mar;252(1):41–51. [PubMed: 23405894]
42. Mandl JN, Liou R, Klauschen F, Vrisekoop N, Monteiro JP, Yates AJ, et al. Quantification of lymph node transit times reveals differences in antigen surveillance strategies of naïve CD4 $^{+}$ and CD8 $^{+}$ T cells. Proc Natl Acad Sci USA. 2012 Oct 30;109(44):18036–41. [PubMed: 23071319]
43. McDaniel MM, Ganusov VV. Estimating Residence Times of Lymphocytes in Ovine Lymph Nodes. Front Immunol. 2019 Jul 16;10:1492. [PubMed: 31379805]
44. McBride DA, Kerr MD, Johnson WT, Nguyen A, Zoccheddu M, Yao M, et al. Immunomodulatory Microparticles Epigenetically Modulate T Cells and Systemically Ameliorate Autoimmune Arthritis. Advanced Science. 2023 Mar 8;2202720. [PubMed: 36890657]
45. Johnson WT, McBride D, Kerr M, Nguyen A, Zoccheddu M, Bollmann M, et al. Immunomodulatory Nanoparticles for Modulating Arthritis Flares. ACS Nano. 2023 Nov 28;acsnano.3c05298.
46. Svensson MND, Doody KM, Schmiedel BJ, Bhattacharyya S, Panwar B, Wiede F, et al. Reduced expression of phosphatase PTPN2 promotes pathogenic conversion of Tregs in autoimmunity. The Journal of Clinical Investigation. 2019 Mar 1;129(3):1193–210. [PubMed: 30620725]
47. Van Den Berg WB, Joosten LAB, Van Lent PLEM. Murine Antigen-Induced Arthritis. In: Cope AP, editor. Arthritis Research [Internet]. Totowa, NJ: Humana Press; 2007 [cited 2023 Aug 23]. p. 243–53. (Walker JM, editor. Methods in Molecular Medicine; vol. 136). Available from: http://link.springer.com/10.1007/978-1-59745-402-5_18
48. Ponchel F, Burska AN, Hunt L, Gul H, Rabin T, Parmar R, et al. T-cell subset abnormalities predict progression along the Inflammatory Arthritis disease continuum: implications for management. Sci Rep. 2020 Feb 28;10(1):3669. [PubMed: 32111870]
49. Gao Y, Dunlap G, Elahee M, Rao DA. Patterns of T-Cell Phenotypes in Rheumatic Diseases From Single-Cell Studies of Tissue. ACR Open Rheumatology. 2021 Sep;3(9):601–13. [PubMed: 34255929]
50. Korn T, Hiltensperger M. Role of IL-6 in the commitment of T cell subsets. Cytokine. 2021 Oct;146:155654. [PubMed: 34325116]
51. Sakaguchi S, Takahashi T, Hata H, Yoshitomi H, Tanaka S, Hirota K, et al. SKG mice, a monogenic model of autoimmune arthritis due to altered signal transduction in T-cells. In: The Hereditary Basis of Rheumatic Diseases. 2006.
52. John S, Shephard N, Liu G, Zeggini E, Cao M, Chen W, et al. Whole-Genome Scan, in a Complex Disease, Using 11,245 Single-Nucleotide Polymorphisms: Comparison with Microsatellites. The American Journal of Human Genetics. 2004 Jul;75(1):54–64. [PubMed: 15154113]
53. MacKay K, Eyre S, Myerscough A, Milicic A, Barton A, Laval S, et al. Whole-genome linkage analysis of rheumatoid arthritis susceptibility loci in 252 affected sibling pairs in the United Kingdom. Arthritis & Rheumatism. 2002 Mar;46(3):632–9. [PubMed: 11920398]

54. Zheng Z, Chang L, Mu J, Ni Q, Bing Z, Zou QH, et al. Database of synovial T cell repertoire of rheumatoid arthritis patients identifies cross-reactive potential against pathogens including unencountered SARS-CoV-2. Ann Rheum Dis. 2023 Mar 1;82(3):438. [PubMed: 36261250]
55. Lutzky V, Hannawi S, Thomas R. Cells of the synovium in rheumatoid arthritis. Dendritic cells. Arthritis Res Ther. 2007;9(4):219. [PubMed: 17850683]
56. Leung BP, Conacher M, Hunter D, McInnes IB, Liew FY, Brewer JM. A Novel Dendritic Cell-Induced Model of Erosive Inflammatory Arthritis: Distinct Roles for Dendritic Cells in T Cell Activation and Induction of Local Inflammation. The Journal of Immunology. 2002 Dec 15;169(12):7071–7. [PubMed: 12471143]
57. Ramos MI, Garcia S, Helder B, Aarrass S, Reedquist KrisA, Jacobsen SE, et al. cDC1 are required for the initiation of collagen-induced arthritis. Journal of Translational Autoimmunity. 2020;3:100066. [PubMed: 33015599]
58. Page G, Lebecque S, Miossec P. Anatomic Localization of Immature and Mature Dendritic Cells in an Ectopic Lymphoid Organ: Correlation with Selective Chemokine Expression in Rheumatoid Synovium. The Journal of Immunology. 2002 May 15;168(10):5333–41. [PubMed: 11994492]
59. Gottschalk RA, Hathorn MM, Beuneu H, Corse E, Dustin ML, Altan-Bonnet G, et al. Distinct influences of peptide-MHC quality and quantity on in vivo T-cell responses. Proc Natl Acad Sci USA. 2012 Jan 17;109(3):881–6. [PubMed: 22223661]
60. Biton J, Saidenberg-Kermanac'h N, Decker P, Boissier MC, Semerano L, Sigaux J. The exposome in rheumatoid arthritis. Joint Bone Spine. 2022 Nov;89(6):105455. [PubMed: 35964886]
61. Potempa J, Mydel P, Koziel J. The case for periodontitis in the pathogenesis of rheumatoid arthritis. Nat Rev Rheumatol. 2017 Oct;13(10):606–20. [PubMed: 28835673]
62. Liu X, Tedeschi SK, Barbhaiya M, Leatherwood CL, Speyer CB, Lu B, et al. Impact and Timing of Smoking Cessation on Reducing Risk of Rheumatoid Arthritis Among Women in the Nurses' Health Studies. Arthritis Care Res. 2019 Jul;71(7):914–24.
63. Sibener LV, Fernandes RA, Kolawole EM, Carbone CB, Liu F, McAffee D, et al. Isolation of a Structural Mechanism for Uncoupling T Cell Receptor Signaling from Peptide-MHC Binding. Cell. 2018 Jul 26;174(3):672–687.e27. [PubMed: 30053426]
64. Choi HK, Cong P, Ge C, Natarajan A, Liu B, Zhang Y, et al. Catch bond models may explain how force amplifies TCR signaling and antigen discrimination. Nat Commun. 2023 May 5;14(1):2616. [PubMed: 37147290]
65. Zareie P, Szeto C, Farenc C, Gunasinghe SD, Kolawole EM, Nguyen A, et al. Canonical T cell receptor docking on peptide–MHC is essential for T cell signaling. Science. 2021 Jun 4;372(6546):eabe9124. [PubMed: 34083463]
66. Hata H, Sakaguchi N, Yoshitomi H, Iwakura Y, Sekikawa K, Azuma Y, et al. Distinct contribution of IL-6, TNF-α, IL-1, and IL-10 to T cell-mediated spontaneous autoimmune arthritis in mice. Journal of Clinical Investigation. 2004;114(4).
67. Ito HO, So T, Ueda T, Imoto T, Koga T. Prevention of collagen-induced arthritis (CIA) by treatment with polyethylene glycol-conjugated type II collagen; distinct tolerogenic property of the conjugated collagen from the native one. Clinical and Experimental Immunology. 2003 Oct 29;108(2):213–9.
68. Kim WU, Lee WK, Ryoo JW, Kim SH, Kim J, Youn J, et al. Suppression of collagen-induced arthritis by single administration of poly(lactic-co-glycolic acid) nanoparticles entrapping type II collagen: A novel treatment strategy for induction of oral tolerance. Arthritis and Rheumatism. 2002;46(4).
69. Allen R, Chizari S, Ma JA, Raychaudhuri S, Lewis JS. Combinatorial, Microparticle-Based Delivery of Immune Modulators Reprograms the Dendritic Cell Phenotype and Promotes Remission of Collagen-Induced Arthritis in Mice. ACS Applied Bio Materials. 2019;2(6).
70. Zhang Q, Dehaini D, Zhang Y, Zhou J, Chen X, Zhang L, et al. Neutrophil membrane-coated nanoparticles inhibit synovial inflammation and alleviate joint damage in inflammatory arthritis. Nature Nanotech. 2018 Dec;13(12):1182–90.
71. Bassin EJ, Buckley AR, Piganelli JD, Little SR. TRI microparticles prevent inflammatory arthritis in a collagen-induced arthritis model. PLOS ONE. 2020 Sep 23;15(9).

72. Lei J, Coronel MM, Yolcu ES, Deng H, Grimany-Nuno O, Hunckler MD, et al. FasL microgels induce immune acceptance of islet allografts in nonhuman primates. Sci Adv. 2022 May 13;8(19):eabm9881. [PubMed: 35559682]

73. Phillips BE, Garciafigueroa Y, Engman C, Liu W, Wang Y, Lakomy RJ, et al. Arrest in the Progression of Type 1 Diabetes at the Mid-Stage of Insulitic Autoimmunity Using an Autoantigen-Decorated All-trans Retinoic Acid and Transforming Growth Factor Beta-1 Single Microparticle Formulation. Front Immunol. 2021 Mar 8;12:586220. [PubMed: 33763059]

74. Iberg CA, Hawiger D. Natural and Induced Tolerogenic Dendritic Cells. The Journal of Immunology. 2020 Feb 15;204(4):733–44. [PubMed: 32015076]

75. Verbeke CS, Gordo S, Schubert DA, Lewin SA, Desai RM, Dobbins J, et al. Multicomponent Injectable Hydrogels for Antigen-Specific Tolerogenic Immune Modulation. Adv Healthcare Mater. 2017 Mar;6(6):1600773.

76. Cho JJ, Stewart JM, Drashansky TT, Brusko MA, Zuniga AN, Lorentsen KJ, et al. An antigen-specific semi-therapeutic treatment with local delivery of tolerogenic factors through a dual-sized microparticle system blocks experimental autoimmune encephalomyelitis. Biomaterials. 2017 Oct;143:79–92. [PubMed: 28772190]

77. Lewis JS, Stewart JM, Marshall GP, Carstens MR, Zhang Y, Dolgova NV, et al. Dual-Sized Microparticle System for Generating Suppressive Dendritic Cells Prevents and Reverses Type 1 Diabetes in the Nonobese Diabetic Mouse Model. ACS Biomater Sci Eng. 2019 May 13;5(5):2631–46. [PubMed: 31119191]

78. Jhunjhunwala S, Balmert SC, Raimondi G, Dons E, Nichols EE, Thomson AW, et al. Controlled release formulations of IL-2, TGF-β1 and rapamycin for the induction of regulatory T cells. Journal of Controlled Release. 2012;159(1).

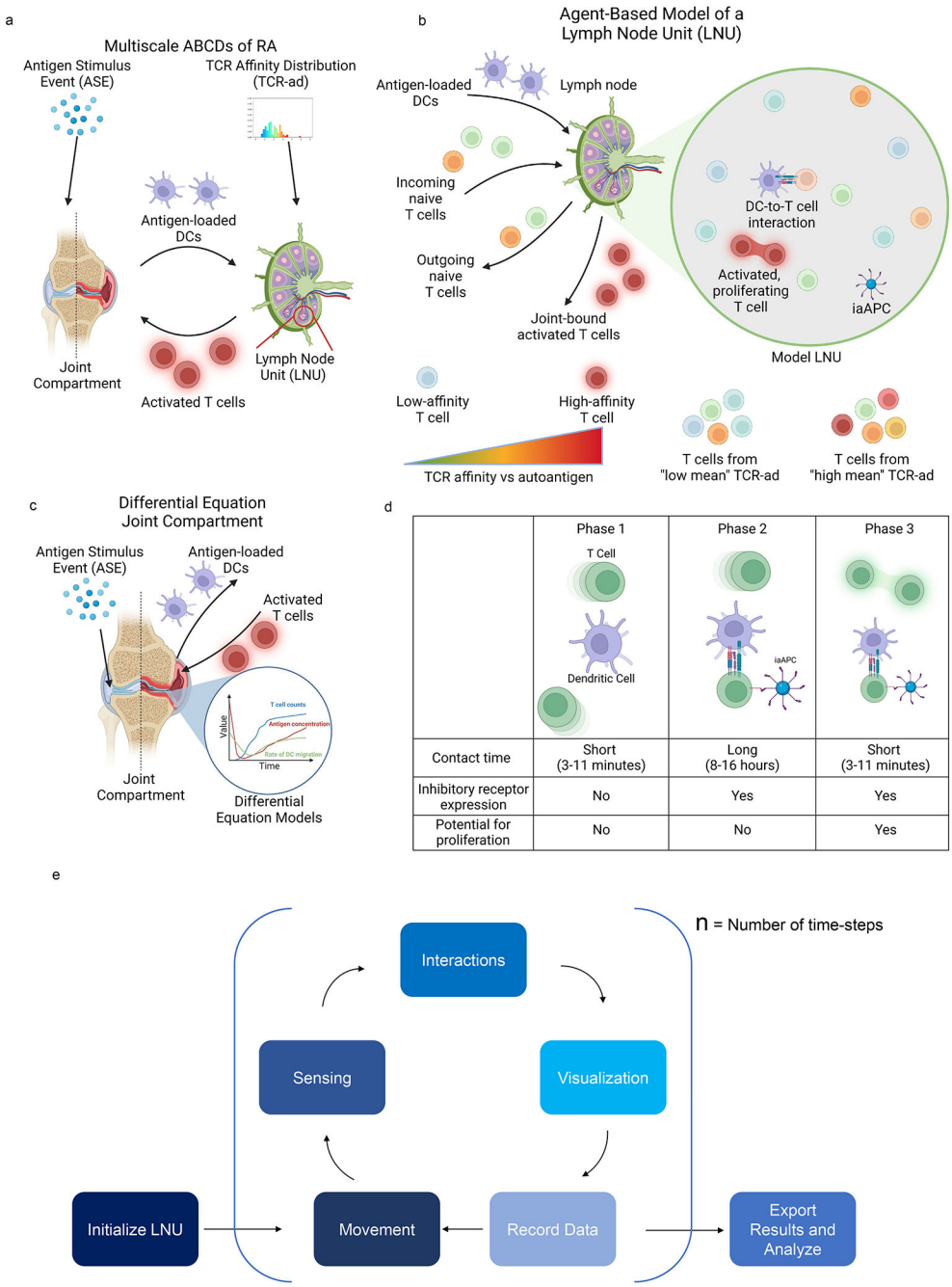

FIGURE 1. Agent-based model of pathogenic T cell proliferation in inflammatory arthritis.

(a) Overview of the multiscale Agent-Based, Cell-Driven model of Inflammatory arthritis (ABCD of IA) depicting the model compartments which include the lymph node unit (LNU) and the joint compartment, and the input parameters consisting of antigen stimulus event (ASE) and T cell receptor affinity distribution (TCR-ad). (b) Schematic of the LNU. T cells and dendritic cells (DCs) enter and exit the LNU and interact within the simulated LNU. LNUs are populated with T cells with affinities to the model antigen that are sampled from a TCR-ad, which is set at the initialization of the simulation. (c) Schematic of the joint

compartment model. T cells and dendritic cells (DCs) enter and exit the joint compartment respectively. (d) The rules governing phases of T cell activation as well as T cell:dendritic cell (DC) and T cell:inhibitory artificial antigen presenting cell (iaAPC) interactions in the model. T cells are activated by receiving a stimulation signal proportional to their T cell receptor (TCR) affinity during contacts with DCs. TCR signaling in phase 2 or phase 3 of activation may be temporarily inhibited by contacts with co-inhibitory molecule presenting iaAPC. (e) Workflow for computational simulation. Upon initiation, all starting cells are generated in the LNU and an initial concentration of antigen is generated in the joint compartment. The algorithm then runs through a cycle of updating the position of cells, sensing and implementing interactions that need to occur based on positions and status of agents, followed by recording data and visualizations for the timestep. The simulation runs for a set amount of timesteps before terminating and compiling the results of the run.

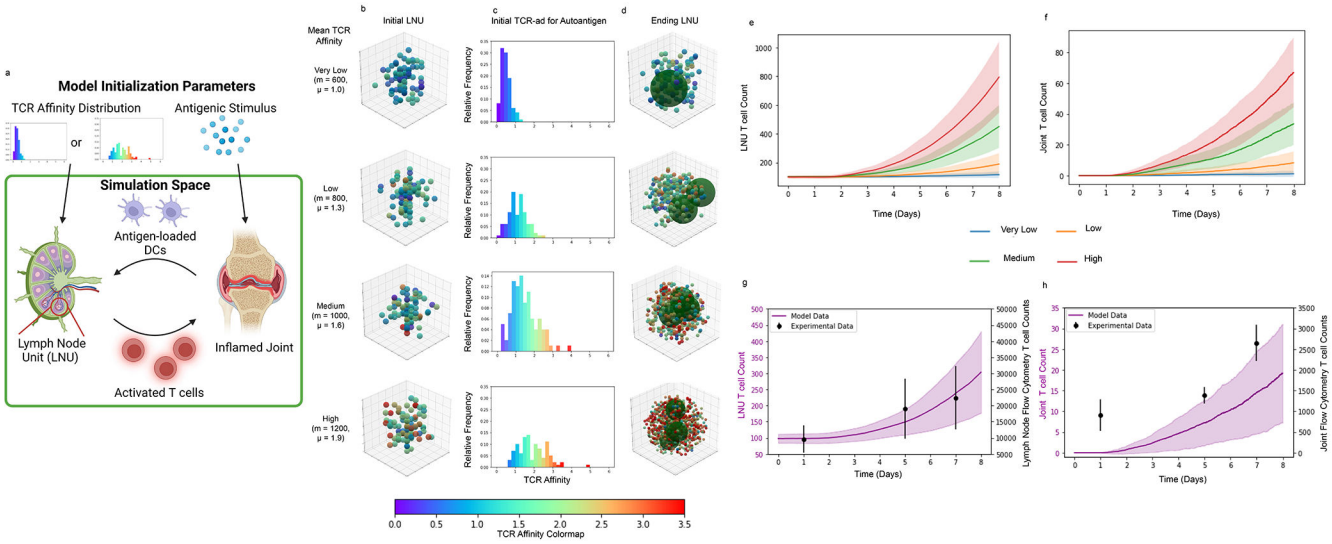

FIGURE 2. TCR-ad influences T cell proliferation dynamics in inflammatory arthritis.

(a) Initialization of the model to test the effect of TCR-ad on T cell proliferation. (b,c) Representative initial (b) visualization and (c) TCR-ad of LNU with TCR affinities sampled from TCR-ad denoted as “Very Low”, “Low”, “Medium” and “High” corresponding to Maxwell-Boltzmann distributions with scale parameter m of 600, 800, 1000, and 1200, respectively, as outlined in Equation 1. (c) Representative final (d) visualization from the LNU depicted in b. (e) T cell counts in LNU from the four representative LNU cases in b-e. (f) Change in T cell counts in the joint compartment over the simulation timeframe. (g) T cell dynamics in LNU with a scale parameter of m = 900 compared to experimental lymph node T cell count dynamics from arthritic SKG mice determined using flow cytometry. (h) T cell dynamics in a model joint compartment with a scale parameter of m = 900 compared to experimental ankle joint T cell counts from arthritic SKG mice determined using flow cytometry. Data in e-h represent the mean (solid line or points) ± s.d. (shading or error bars) of n = 100 trials per condition for model results and n = 4 mice for in vivo results. Reference data in g, h were obtained from prior work.(44,45)

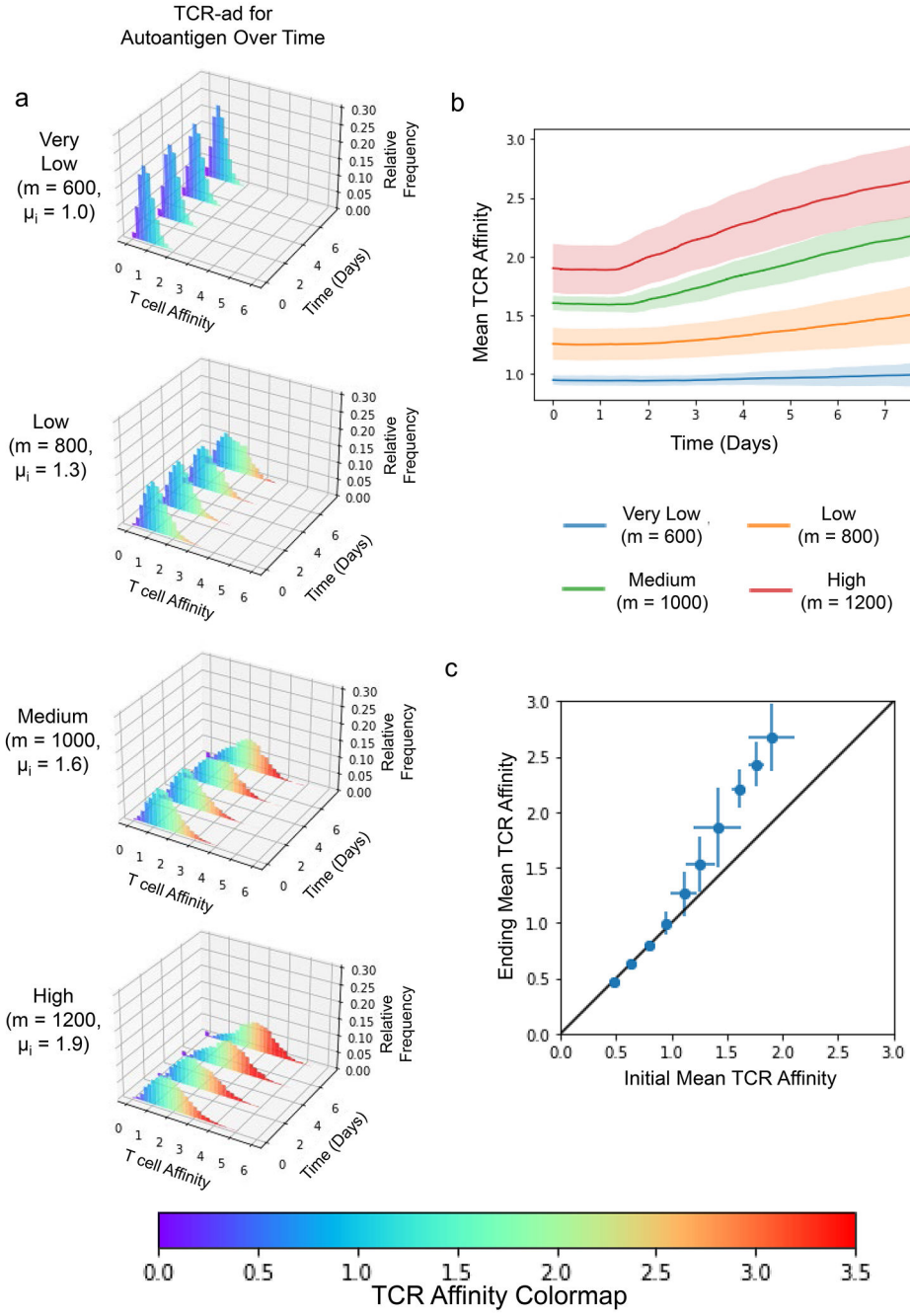

FIGURE 3. TCR-ad in the LNU changes with T cell proliferation.

(a) Change in TCR-ad over the simulation timeframe for lymph node distributions denoted as “Very Low”, “Low”, “Medium” and “High” as in Figure 2. (b) Mean TCR-ad over time for LNUs initialized with various Maxwell-Boltzmann distribution scale parameters used in Figure 1, denoted in the figure legend. (c) Initial vs ending TCR-ad for LNUs initialized with various Maxwell-Boltzmann distribution scale parameters spanning 300-1200. Data in b represent the mean (solid line) ± s.d. (shading) of n = 100 trials per condition. Data in c represents the mean ± s.d. (error bars) of n = 100 trials per condition.

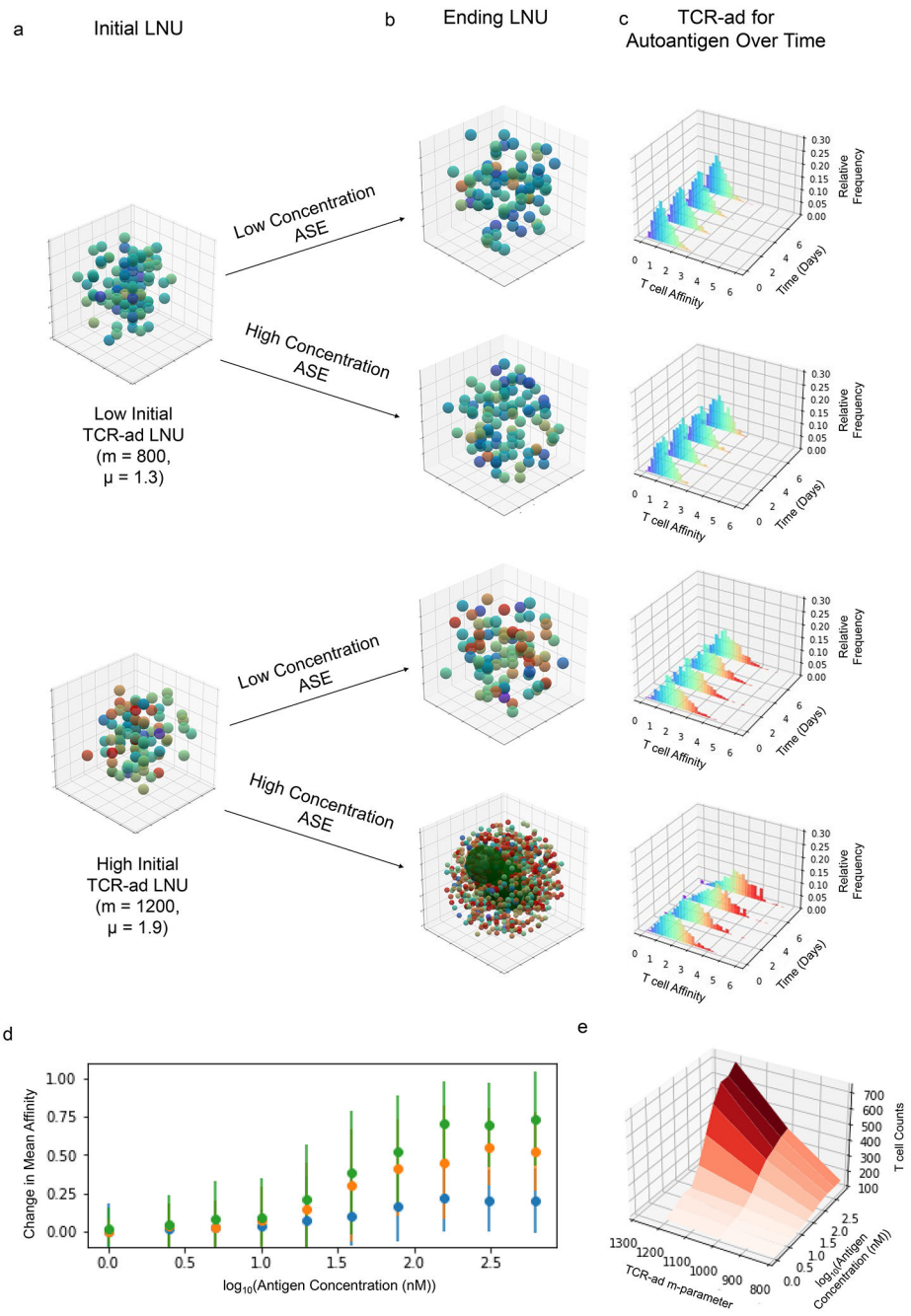

FIGURE 4. Antigen concentration during initiating ASE influences inflammatory state.
(a,b) (a) Initial and (b) final representative LNU visualizations for high and low mean TCR-ad initialized at high and low antigen concentrations. (c) Change in TCR-ad over the simulation timeframe for average LNUs from conditions represented in a and b. (d) The change in the mean value of the TCR-ad relative to the $\log_{10}$ antigen concentration in nanomolar. (e) Contour map of T cell proliferation, measured by T cells in the LNU at the end of 8 days, as a function of the Maxwell-Boltzmann distribution scale parameter, m, and the $\log_{10}$ of the initiating ASE antigen concentration. Data in d represent the mean ± s.d.

(error bars) of n = 100 trials per condition. Data in e represent the mean of n = 100 trials per condition.

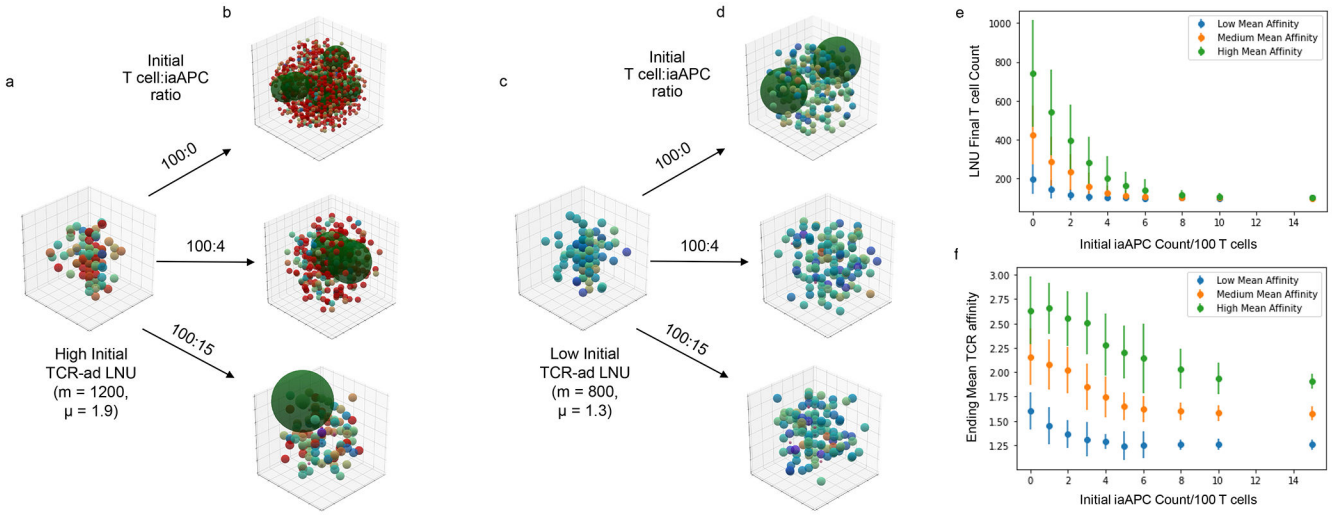

FIGURE 5. Inhibitory artificial antigen presenting cells control transition to chronically inflamed state.

(a,b) Representative (a) initial and (b) final visualizations for high mean TCR-ad LNU over a range of T cell:iaAPC ratios. (c,d) Representative (c) initial and (d) final visualizations for low mean TCR-ad LNU over a range of T cell:iaAPC ratios. (e) LNU final T cell counts plotted as a function of initial concentration of iaAPCs across multiple TCR-ad. (f) Ending mean value of the TCR-ad for LNUs initialized with TCR-ad across a range of affinity distributions and initial T cell:iaAPC ratios. Data in e and f represent the mean ± s.d. (error bars) of n = 100 trials per condition.

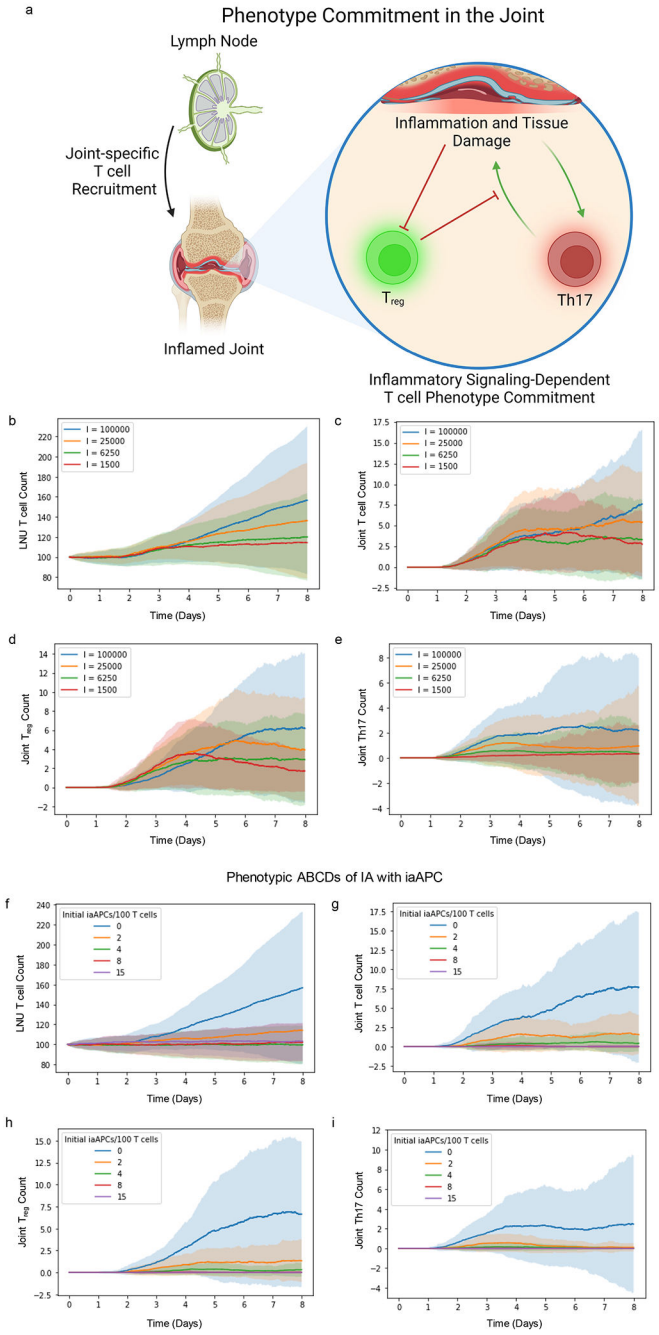

FIGURE 6. The cytokine milieu in the joint microenvironment drives transition to chronic inflammation over resolution.

(a) Schematic for a model of T cell phenotype commitment in the joints. (b) T cell counts in LNU at a range of initial Th17-inducing cytokine levels. (c) Total T cell counts, (d) T_{reg} and (e) Th17 counts in the joint at the corresponding Th17-inducing cytokine levels. (f) T cell counts in LNU at the maximum concentration of Th17-inducing cytokine levels in b at various initial iaAPC:T cell ratios (g) Total T cell counts, (h) T_{reg} and (i) Th17 counts in the joint at the maximum concentration of Th17-inducing cytokine levels in c-e at various

initial iaAPC:T cell ratios. Data in b-i represent the mean ± s.d. (shading) of n = 100 trials per condition.

Table 1.

Key simulation initialization parameters

Parameters	Values	Source/Method
Voxel Size	216 μm^3	Bogle (2010) ref [36]
Simulation time (t)	8 days	N/A
Probability of T cell egress/ingress during timestep (P_T)	0.00017	Mandl (2012), McDaniel (2019) refs [42, 43]
Initial T cell count (nT)	100	N/A
TCR Affinity Distribution Parameter (m)	300-1200	Parameter Sweep
Initial Antigen Concentration Following ASE (a_0)	1-40000 nM	Parameter Sweep, Van Den Berg (2007) ref [47]
Initial T cell:iaAPC ratio (r)	1-15	Parameter Sweep